

Remarkable Solar Thermochemical CO₂ Splitting Performances

based on Ce- and Al- doped SrMnO₃ Perovskites

Ke Gao¹, Xianglei Liu^{1,2,3*}, Qi Wang¹, Zhixing Jiang¹, Cheng Tian¹, Nan Sun¹,
Yimin Xuan^{1,2,3}

¹ School of Energy and Power Engineering, Nanjing University of Aeronautics and
Astronautics, Nanjing, Jiangsu Province, 210016, China

² Key Laboratory of Thermal Management and Energy Utilization of Aviation
Vehicles, Ministry of Industry and Information Technology,
Nanjing, Jiangsu Province, 210016, China

³ Integrated Energy Institute, Nanjing University of Aeronautics and
Astronautics, Nanjing, Jiangsu Province, 210016, China

*Corresponding author, E-mail: xliu@nuaa.edu.cn

This word file includes:

Fig. S1 Preparation procedures of perovskite powder samples.

Fig. S2 The convergence trend of total energy with different cutoff.

Fig. S3 Temperature varies with the concentration ratio for different samples.

Fig. S4 SEM images of remaining Ce- doped SrMnO₃ at A site.

Fig. S5 Particle size distribution of Ce- doped SrMnO₃ before and after cycles.

Fig. S6 The X-ray diffraction patterns of cycled Al- doped Sr_{0.6}Ce_{0.4}MnO₃.

Fig. S7 XPS profile for (a) Ce 3d and (b) Al 2p spectra for SCMA20.

Fig. S8 Particle size distribution of Al- doped Sr_{0.6}Ce_{0.4}MnO₃ before and after cycles.

Fig. S9 SEM mapping of SCMA20 before and after cycling.

Fig. S10 The DFT calculation model for initial and final positions.

Fig. S11 Total CO₂ conversion rate and real-time O₂ production rate profiles for
SCMA20 of 20 cycles.

Fig. S12 Particle size distribution of SCMA20 after 20 redox cycles.

Fig. S13 Temperature schemes designed for solar thermochemical CO₂ splitting
within different reduction temperatures.

Fig. S14 The SEM image of SCMA20 at 1400 °C reduction temperature.

Tab. S1 Detail O₂ and CO yields of SCMA20 in last three cycles within different
reduction temperatures.

Tab. S2 Detailed performance comparison of different redox powder materials in this

work with other literature reports.

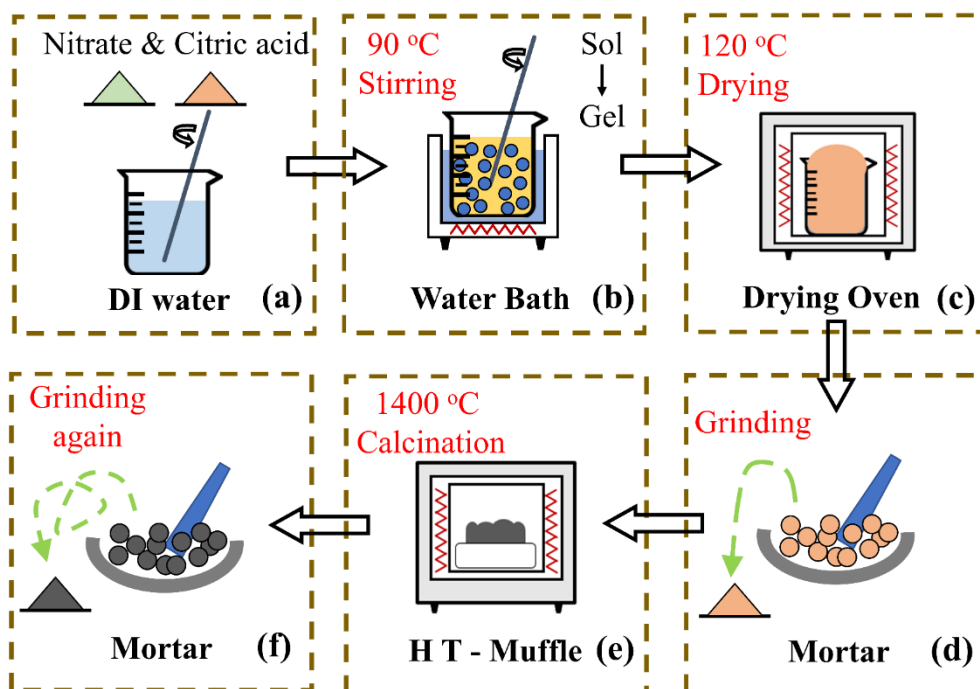


Fig. S1 Preparation procedures of perovskite powder samples.

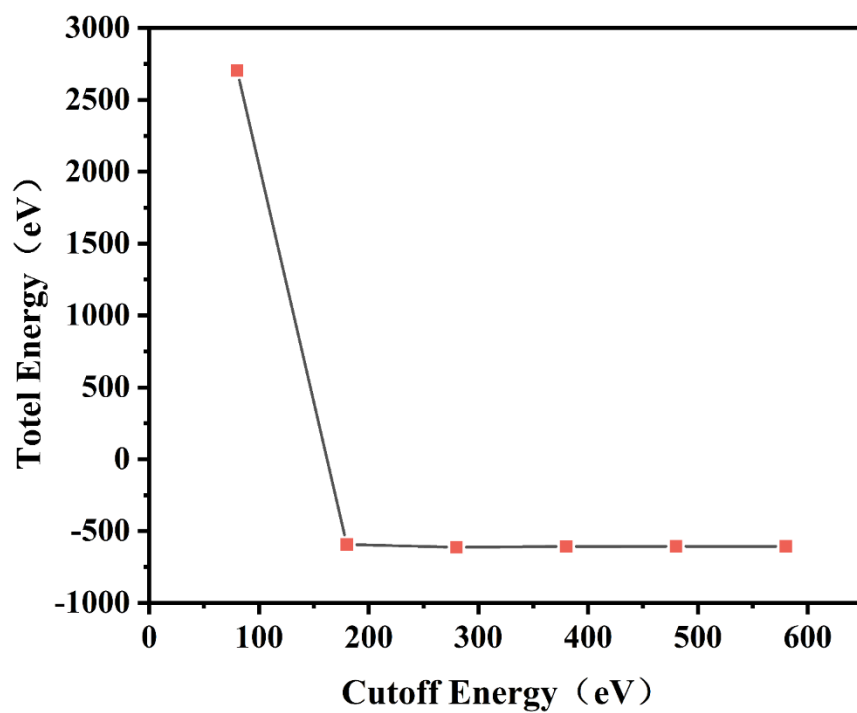


Fig. S2 The convergence trend of total energy with different cutoff.

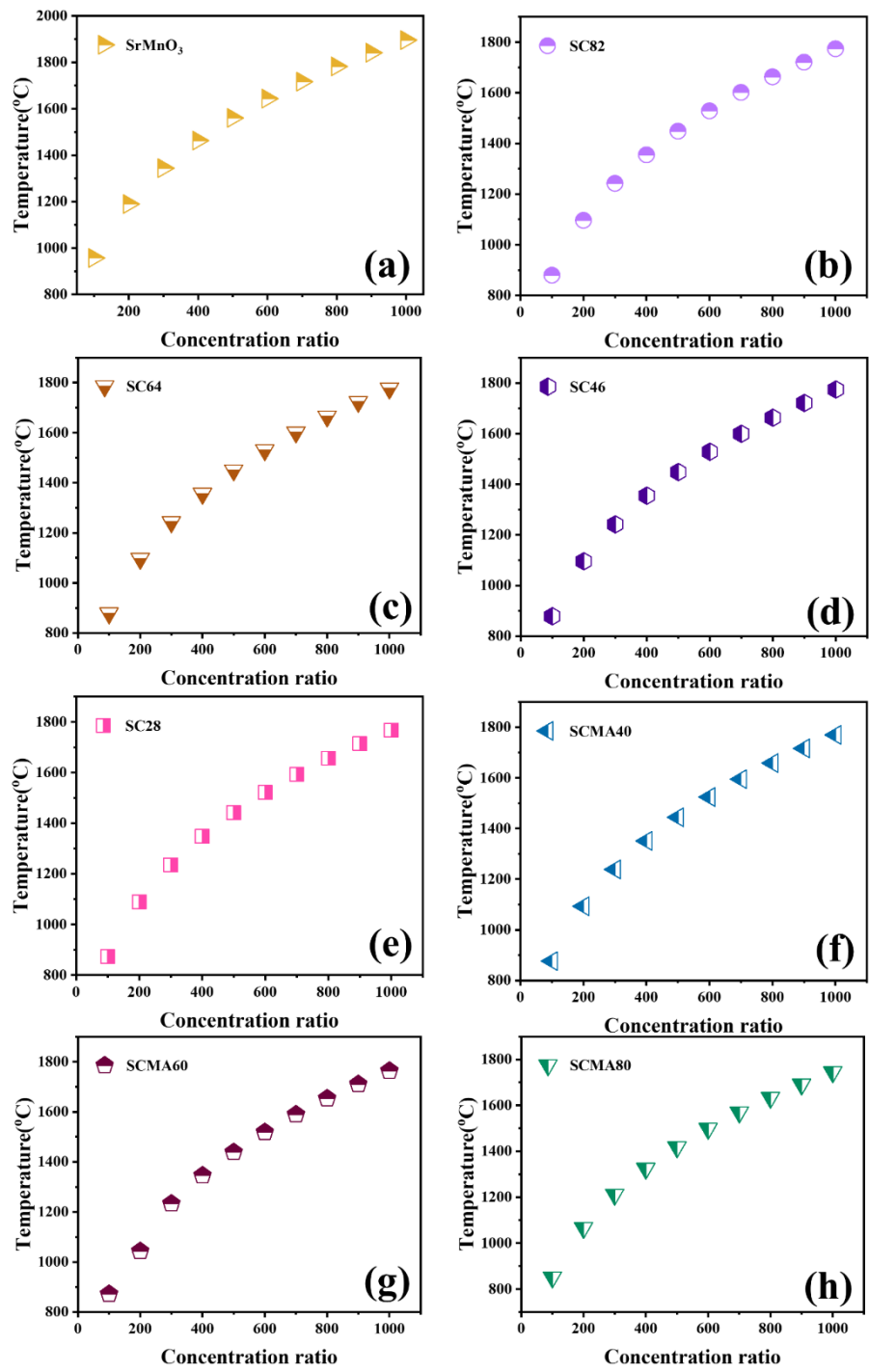


Fig. S3 Temperature varies with the concentration ratio for different samples.

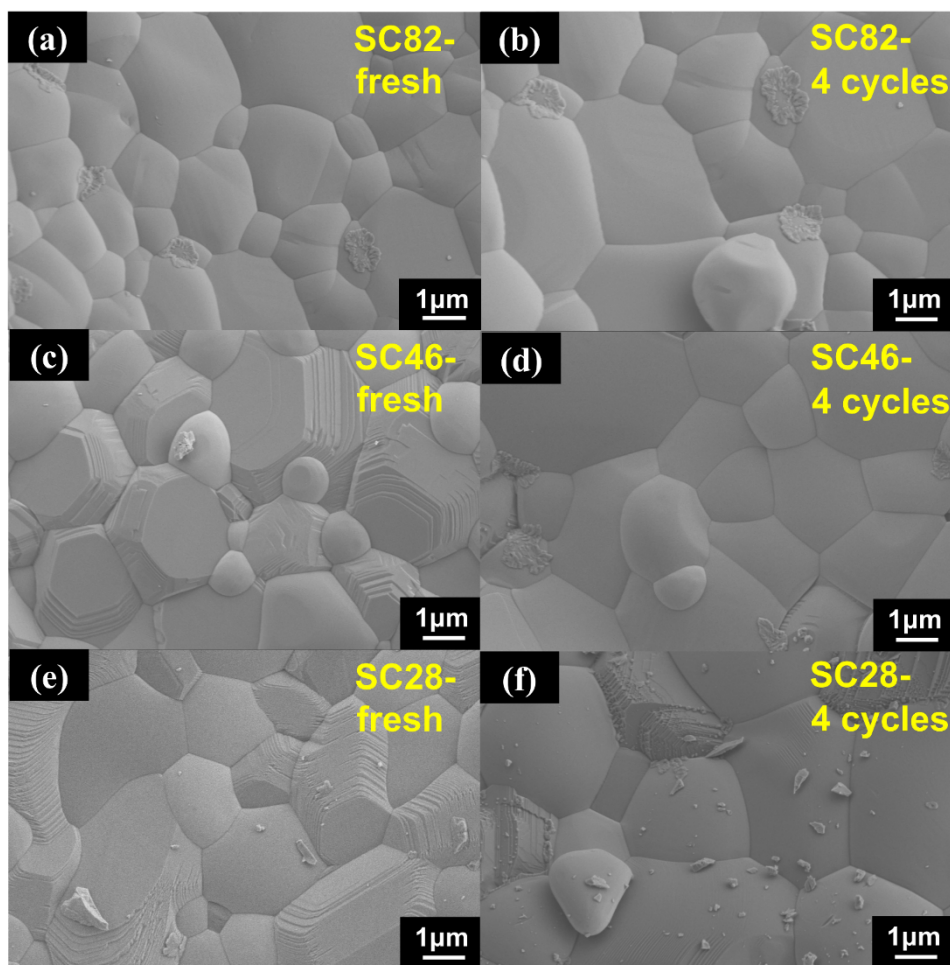


Fig. S4 SEM images of remaining Ce- doped SrMnO₃ at A site.

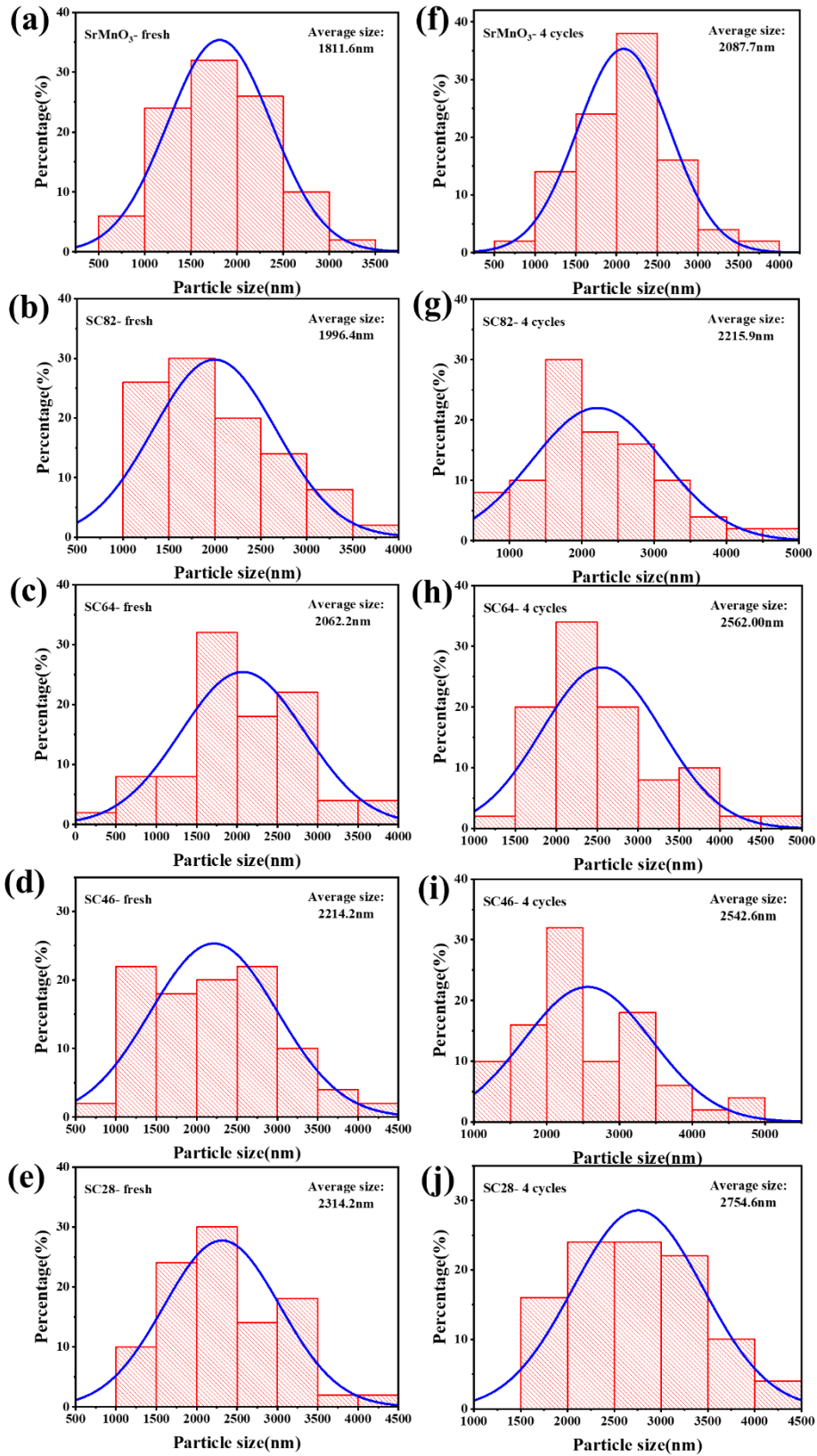


Fig. S5 Particle size distribution of Ce- doped SrMnO₃ before and after cycles.

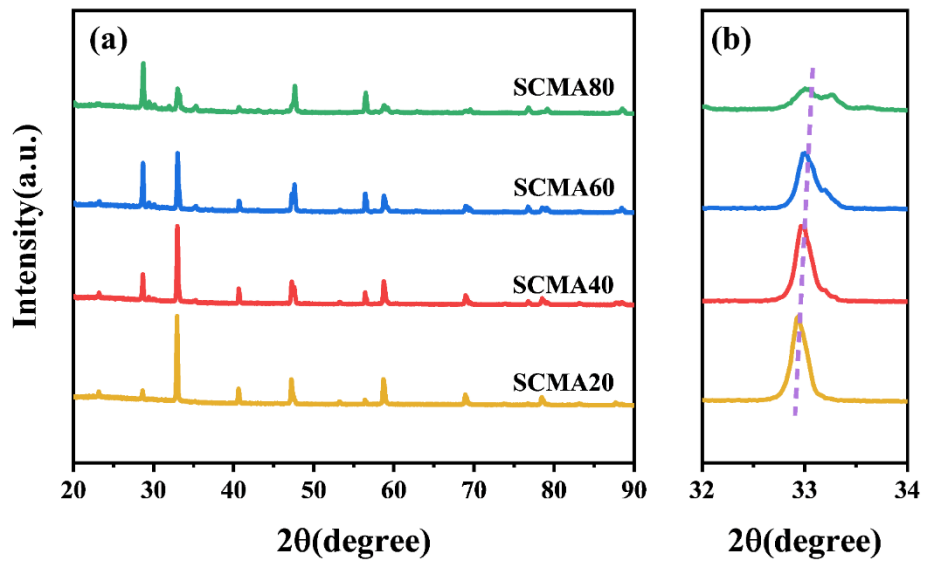


Fig. S6 X-ray diffraction patterns of cycled Al- doped $\text{Sr}_{0.6}\text{Ce}_{0.4}\text{MnO}_3$.

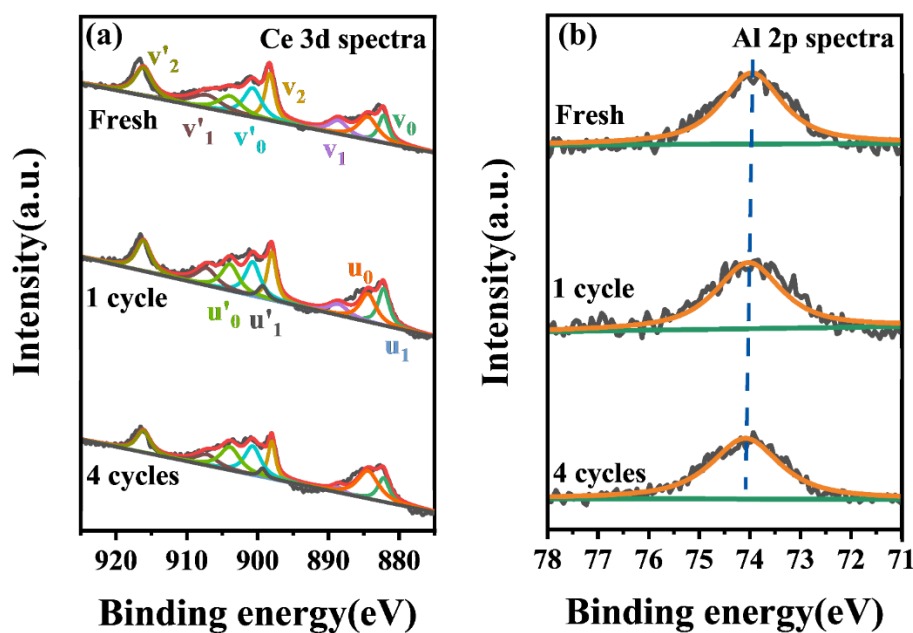


Fig. S7 XPS profile for (a) Ce 3d and (b) Al 2p spectra for SCMA20.

Fig. S7a shows Ce 3d spectra of the fresh, after one cycle, and after four cycles for SCMA20. Ce 3d spectra (Ce 3d_{5/2} and Ce 3d_{3/2}) been divided into ten convolved peaks. Ce⁴⁺ has been fitted with six peaks: v₀ (882.2 eV), v₁ (888.6 eV), v₂ (898 eV), v'₀ (900.7 eV), v'₁ (907.2 eV), and v'₂ (916.2 eV). Meanwhile, Ce³⁺ has been fitted with four peaks: u₀ (884.4 eV), u₁ (880.6 eV), u'₀ (903.9 eV), and u'₁ (899.3 eV).^{1, 2} It has been reported that the presence of Ce³⁺ shows the formation of oxygen vacancies, and the number of Ce³⁺ represents the concentration of oxygen vacancies in CeO₂.^{3, 4} By calculation, the concentration of Ce³⁺ on SCMA20 is gradually increasing with the increase of cycle numbers, and the value of Ce³⁺/(Ce³⁺ + Ce⁴⁺) increases from 0.26 to 0.30 to 0.41, showing oxygen vacancies increasing after cycling. This phenomenon can be attributed to the sample being exposed to high temperature. Meanwhile, as shown in Fig. S7b, the peak position of Al 2p is unchanged (around 74.1 eV) before and after cycling.^{5, 6} Therefore, there is no obvious change of Al 2p spectra for SCMA20 after cycling, showing the good stability on SCMA20.

Reference :

- 1 E. Beche, P. Charvin, D. Perarnau, S. Abanades and G. Flamant, *Surf. Interface Anal.*, 2008, **40**, 264-267.

- 2 H. Shi, C. Tian, X. Liu and N. Sun et al., *Chem. Eng. J.*, 2023, **454**, 140063.
- 3 D. He, H. Hao, D. Chen, J. Liu, J. Yu, J. Lu, F. Liu, G. Wan, S. He, Y. Luo, *Catal. Today*, 2017, **281**, 559-565.
- 4 H. Ay, D. Üner, *Appl. Catal. B*, 2015, **179**, 128-138.
- 5 N.M. Figueiredo, N.J.M. Carvalho, A. Cavaleiro, *Appl. Surf. Sci.*, 2011, **257**, 5793-5798.
- 6 K.J. Kim, J.S. Jang, *Anal. Chem.*, 2009, **81**, 8519-8522.

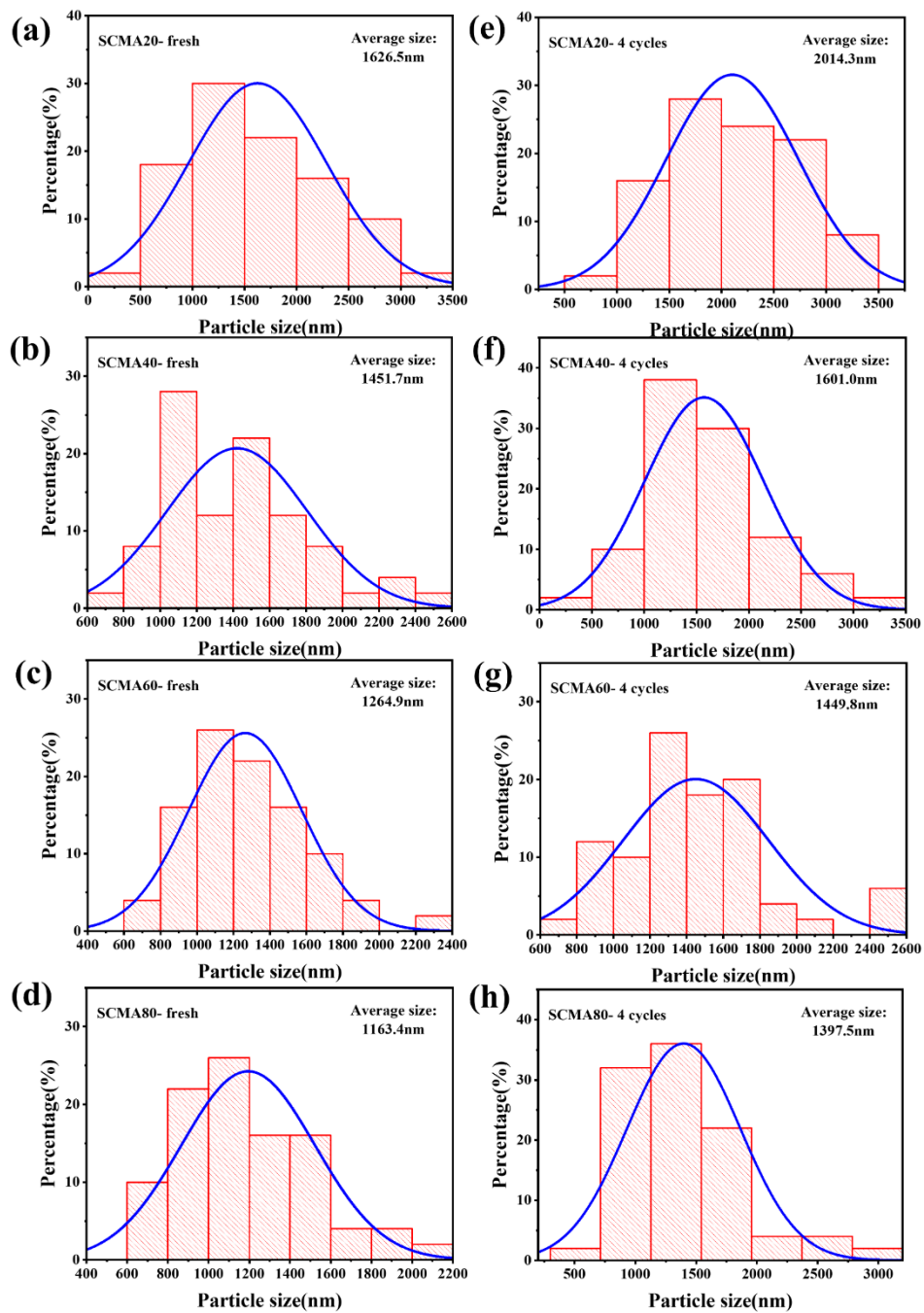


Fig. S8 Particle size distribution of Al-doped $\text{Sr}_{0.6}\text{Ce}_{0.4}\text{MnO}_3$ before and after cycles.

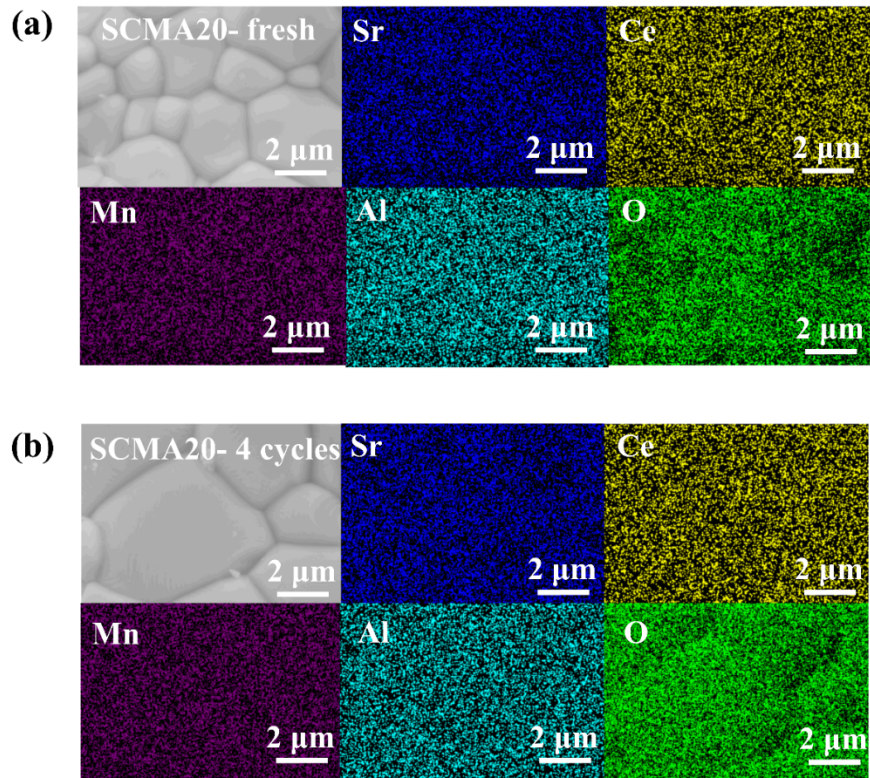


Fig. S9 SEM mapping of SCMA20 before and after cycling.

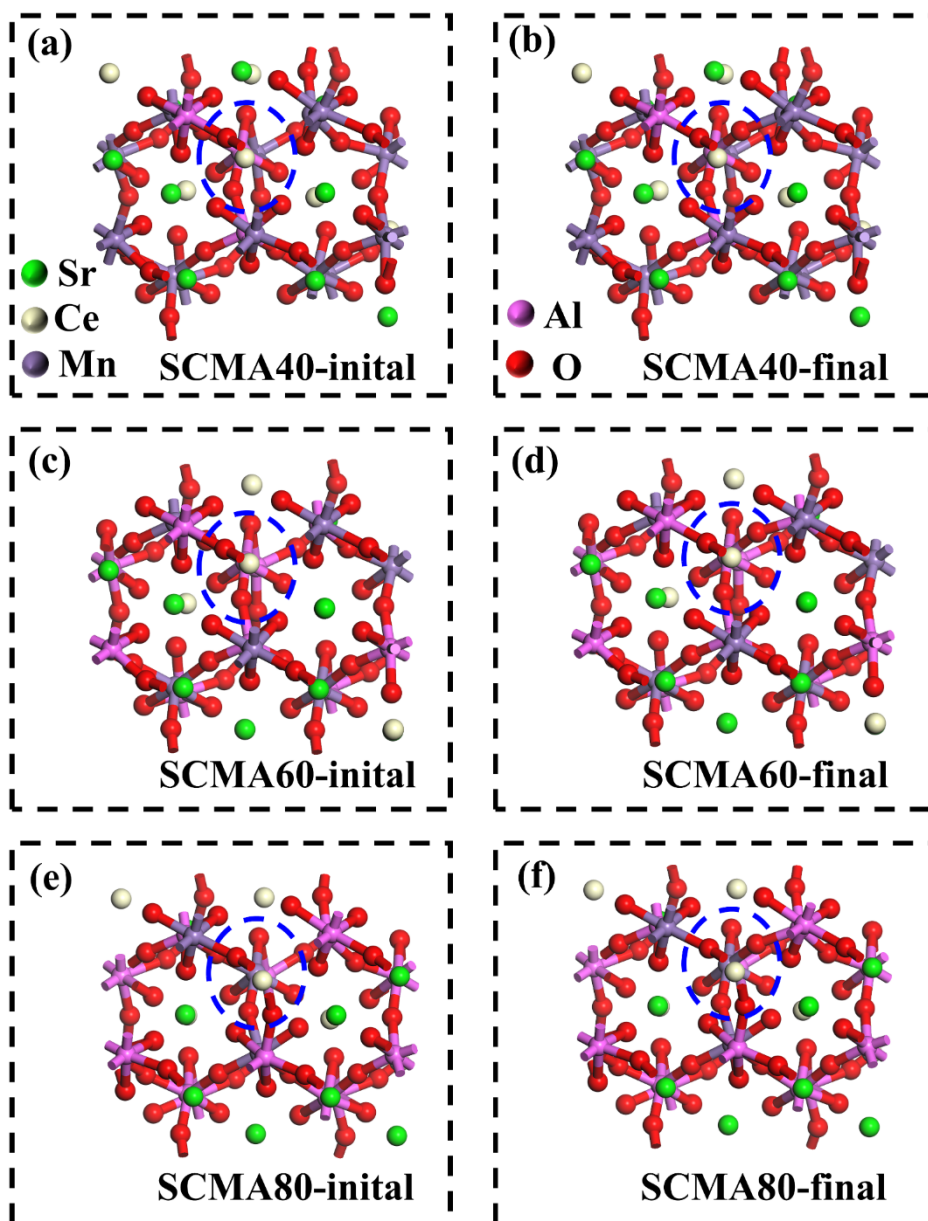


Fig. S10 The DFT calculation model for initial and final positions.

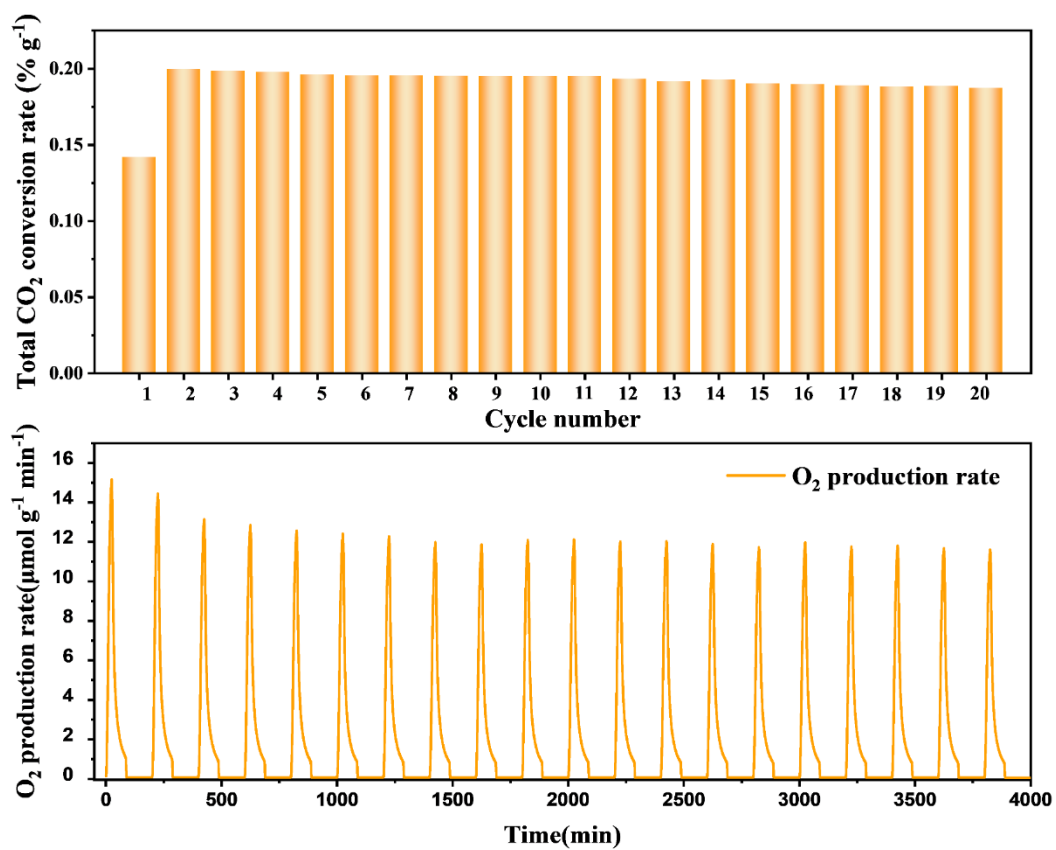


Fig.S11 (a) Total CO₂ conversion rate and real-time O₂ production rate profiles for SCMA20 of 20 cycles.

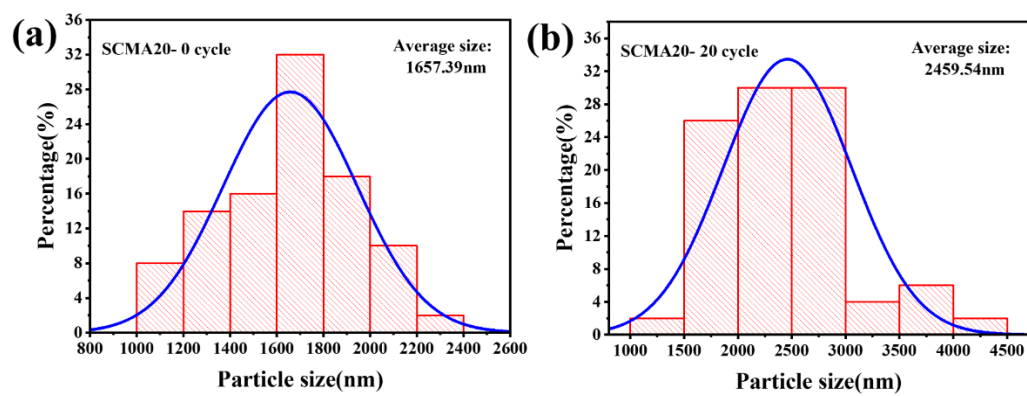


Fig. S12 Particle size distribution of SCMA20 after 20 redox cycles.

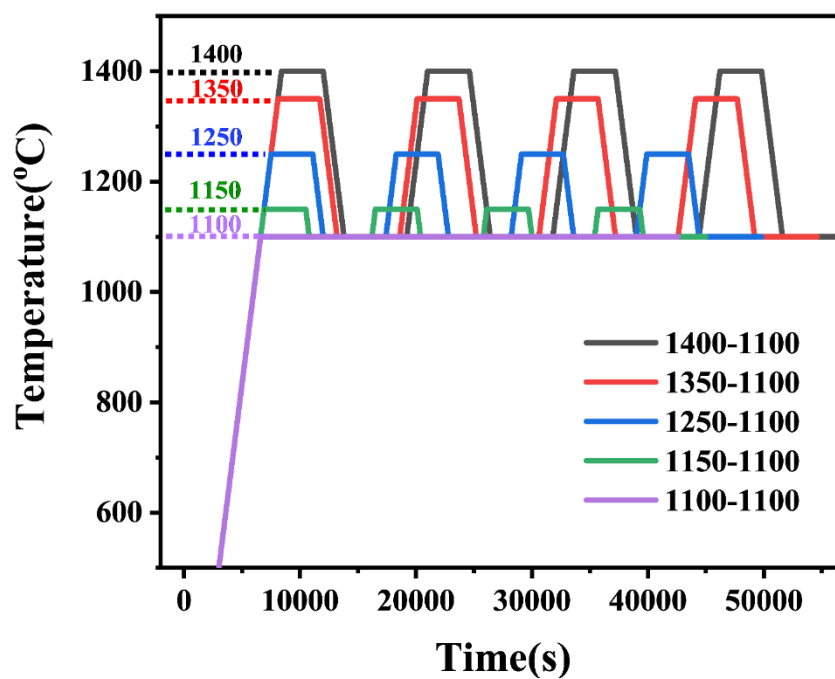


Fig. S13 Temperature schemes designed for solar thermochemical CO₂ splitting within different reduction temperatures.

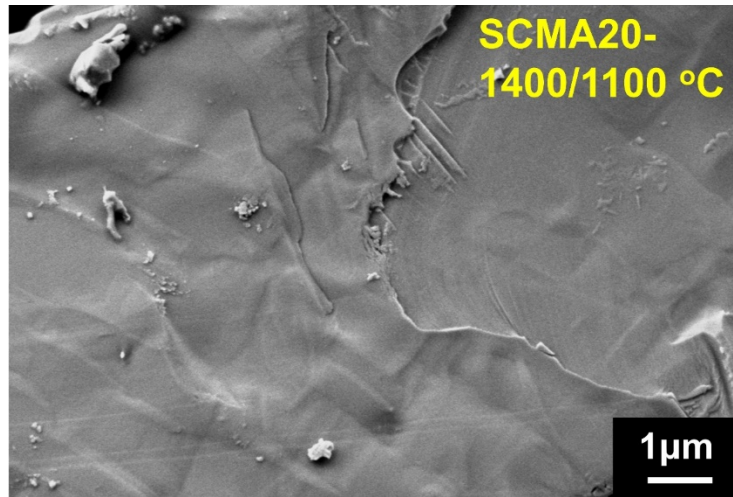


Fig. S14 The SEM image of SCMA20 at 1400 °C reduction temperature.

Tab. S1 Detail O₂ and CO yields of SCMA20 in last three cycles within different reduction temperatures.

Reaction Temperature (°C)	Yield (μmol g ⁻¹)					
	Cycle 2		Cycle 3		Cycle 4	
	O ₂	CO	O ₂	CO	O ₂	CO
1100-1100	60.43	73.31	54.74	80.06	52.82	80.84
1150-1100	97.17	142.29	84.94	145.09	82.61	145.72
1250-1100	224.83	403.69	208.41	399.17	205.93	396.91
1350-1100	495.57	801.27	452.66	798.34	443.93	798.39
1400-1100	531.86	650.26	473.21	698.61	432.96	674.71

The O₂ and CO yields remain basically stable over the last three cycles except for a slight swing for the first cycle. Thus, the total O₂ and CO yields in last three cycles are discussed and analyzed here.

Tab. S2 Detailed performance comparison of different redox powder materials in this work with other literature reports.

Materials	T_{red} (°C)	T_{ox} (°C)	ΔT (°C)	CO yield ($\mu\text{mol g}^{-1}$)	CO peak production rate ($\mu\text{mol g}^{-1} \text{s}^{-1}$)	Measurement method	Cycle number	Average solar absorptance (%)	Ref.
$\text{Sr}_{0.6}\text{Ce}_{0.4}\text{Mn}_{0.8}\text{Al}_{0.2}\text{O}_3$	1350	1100	250	799.34	0.607	Direct	20	87.98	This work
$\text{La}_{0.6}\text{Ca}_{0.4}\text{Mn}_{0.8}\text{Ga}_{0.2}\text{O}_3$	1350	1050	300	513.00	0.464	Direct	8	87.40	[35]
$\text{La}_{0.6}\text{Sr}_{0.4}\text{Mn}_{0.25}\text{Cr}_{0.75}\text{O}_3$	1400	1400	0	312.00	0.595	Direct	15	–	[38]
$\text{Sm}_{0.6}\text{Ca}_{0.4}\text{Mn}_{0.8}\text{Al}_{0.2}\text{O}_3$	1350	1100	250	595.56	0.446	Direct	30	87.10	[47]
$\text{Sm}_{0.6}\text{Sr}_{0.4}\text{MnO}_3$	1300	1300	0	376.10	0.089	Direct	14	86.60	[49]
$\text{LaF}_{0.75}\text{Co}_{0.25}\text{O}_3$	1300	1000	300	117	–	TGA	2	–	[10]
$\text{La}_{0.5}\text{Sr}_{0.5}\text{Fe}_{0.5}\text{Mn}_{0.5}\text{O}_3$	1300	1000	300	107	–	TGA	2	–	[10]
$\text{La}_{0.5}\text{Sr}_{0.5}\text{Co}_{0.5}\text{Mn}_{0.5}\text{O}_3$	1300	1050	250	152.00	–	TGA	2	–	[10]
$\text{La}_{0.6}\text{Sr}_{0.4}\text{FeO}_3$	1200	1050	150	53.00	–	TGA	2	–	[10]
SrFeO_3	1200	1000	200	86.00	–	TGA	2	–	[10]
$\text{SrFeO}_3(\text{SFO-1})$	1100	1000	100	82.50	–	TGA	2	–	[10]
$\text{Ba}_{0.5}\text{Sr}_{0.5}\text{FeO}_3$	1000	1000	0	31.00	–	TGA	2	–	[10]
$\text{Y}_{0.5}\text{Sr}_{0.5}\text{MnO}_3$	1400	900	500	757.00	–	TGA	3	–	[19]
$\text{Y}_{0.5}\text{Sr}_{0.5}\text{MnO}_3$	1300	900	400	524.00	–	TGA	3	–	[19]
$\text{Y}_{0.5}\text{Ca}_{0.5}\text{MnO}_3$	1400	1100	300	671.00	–	TGA	3	–	[19]
$\text{La}_{0.5}\text{Sr}_{0.5}\text{MnO}_3$	1400	1100	300	325.00	–	TGA	3	–	[20]
SrMnO_3	1250	1000	250	511.00	–	TGA	5	–	[22]
$\text{La}_{0.75}\text{Sr}_{0.25}\text{MnO}_3$	1250	1000	250	311.00	–	TGA	5	–	[22]
LaMnO_3	1000	1000	0	223.90	–	TGA	4	–	[22]
$\text{La}_{0.5}\text{Sr}_{0.5}\text{MnO}_3$	1000	1000	0	76.30	–	TGA	4	–	[22]

$\text{La}_{0.5}\text{Sr}_{0.5}\text{MnO}_3$	1000	700	300	134.00	–	TGA	4	–	[22]
$\text{La}_{0.6}\text{Sr}_{0.4}\text{Mn}_{0.4}\text{Al}_{0.6}\text{O}_3$	1350	1000	350	247.00	0.832	TGA	80	–	[23]
CeO_2	1400	1000	400	105.00	–	TGA	3	–	[24]
$\text{Ce}_{0.75}\text{Zr}_{0.25}\text{O}_2$	1400	1050	350	323.90	–	TGA	3	–	[24]
CeO_2	1300	800	500	55.86	–	TGA	3	–	[42]
$\text{La}_{0.9}\text{Sr}_{0.1}\text{CoO}_3$	1300	800	500	90.56	–	TGA	3	–	[42]
$\text{LaCo}_{0.7}\text{Zr}_{0.3}\text{O}_3$	1400	900	500	1066.60	–	TGA	3	–	[42]
